UNIVERSITEIT
AMSTERDAM

VU Research Portal

Series of maxima in the field dependent magnetic moment of layered superconductors

Brongersma, S.H.; de Groot, D.G.; Griessen, R.; Ivlev, B.I.; Koeman, N.J.; Verweij, E.

document version
Publisher's PDF, also known as Version of record

Link to publication in VU Research Portal

citation for published version (APA)
Brongersma, S. H., de Groot, D. G., Griessen, R., Ivlev, B. I., Koeman, N. J., & Verweij, E. (1993). Series of maxima in the field dependent magnetic moment of layered superconductors. *Physical Review Letters*, *71*(14), 2319-2322. https://doi.org/10.1103/PhysRevLett.71.2319

Series of Maxima in the Field Dependent Magnetic Moment of Layered Superconductors

S. H. Brongersma, E. Verweij, N. J. Koeman, D. G. de Groot, and R. Griessen

Free University, Faculty of Physics and Astronomy, De Boelelaan 1081, 1081 HV Amsterdam, The Netherlands

B. I. Ivlev

Landau Institute for Theoretical Physics, Kosygin St. 2, 117940, Moscow, Russia

Magnetic moment measurements on niobium/copper multilayers by means of a torque magnetometer exhibit a series of maxima at specific field strengths H_N when the applied magnetic field makes a small angle with the plane of the superconducting layers. These maxima are shown to be closely related to rearrangements of the parallel vortex system, during which an increasing number of vortex chains is formed in the sample.

Over the last few years intrinsic pinning of vortices in layered superconductors has been widely discussed [1-4]. An interesting consequence of this effect is the possibility of a kinked vortex structure [5-8] when a magnetic field H is applied almost parallel to the layered structure. The vortices consist of long in-plane parts separated by short kinks making a kink angle θ_k with the superconducting planes [(x,y) plane] that is larger than the mean tilt angle θ. One expects then that the sublattice formed by these in-plane parts governs the entering of vortices into a layered material. The in-plane parts of the vortices will thereby also control the magnitude of the in-plane critical current j_c, which is directly proportional to the magnetic moment M_z, due to the kinks. Consequently, one expects to see characteristic features in the field dependence of M_z whenever the configuration of the in-plane vortex system changes. The possibility of such a configuration change is substantiated by early experiments of Guimpel et al. [9] on *thick* Nb/Cu multilayers showing one peak above H_{c1} in the field dependence of the flux expulsion of a magnetic field parallel to the (x,y) plane. It corresponds to the field where the vortex-vortex interaction becomes important and vortices, which above H_{c1} had distributed themselves along the x axis in the middle of the sample, start to form a two-dimensional array. On the basis of Monte Carlo simulations described below we come to the conclusion that not only one peak but a whole series of peaks should be observable in *thin* Nb/Cu multilayers (i.e., where the penetration depth λ_{xy} is larger than the total thickness D of the multilayer). The regime $\lambda_{xy} > D$ can be realized in multilayers with individual layer thicknesses $d \cong \xi_z$, where ξ_z is the coherence length parallel to the z axis [10]. In Nb/Cu multilayers this implies $d \cong 10$ and $D < 400$ nm. In this Letter we report on the observation of series of maxima (in some samples up to six) in M_z when H is increased from H_{c1} to H_{c2}, and show that these maxima are closely related to specific (field dependent) multichain configurations of the in-plane vortices.

Niobium/copper multilayers are grown on sapphire substrates (Al_2O_3 $1\bar{1}02$) at ambient temperatures in a two-electron-gun UHV evaporation chamber. During deposition at a rate of 0.15 nm/s, the base pressure of 10^{-8} Pa increases only to $\sim 10^{-7}$ Pa. Several techniques are used for characterization of the samples. First and second order Bragg peaks as well as low angle diffraction at the interfaces are observed by means of θ-2θ x-ray diffraction (XRD). Rutherford backscattering measurements confirm the periodic structure while the obtained layer thicknesses agree within a few percent with those found from XRD and quartz crystal thickness monitors. The thirty multilayers that have been investigated, with thicknesses ranging from $D = 120$ to $D = 400$ nm, all exhibit series of maxima that can be explained by the *same* mechanism. For a quantitative comparison with calculations we consider here, however, only the data for one sample with an internal structure consisting of fifteen alternately deposited layers of 10 nm Cu and 10 nm Nb, covered by outer copper layers of 50 nm that prevent surface superconductivity. The surface area is 0.75×10 mm^2 along the x and y axes, respectively. Transport measurements with a standard four point technique give a critical temperature of $T_c = 6.0$ K and an anisotropy of $\xi_{xy}/\xi_z = 1.23$ which are both confirmed by the data obtained in torque experiments. Since the in-plane coherence length is $\xi_{xy} = 16.1 \pm 1.7$ nm [11] we thus have $\xi_z = 13.1$ nm.

A capacitance torque magnetometer with a sensitivity of 10^{-9} N m is used for the determination of the magnetic moment of the multilayers [12]. It fits into a helium bath cryostat which is placed in a 1.5 T electromagnet with an angular resolution of 0.05°. A typical measurement with $\theta = 1°$ and the field almost parallel to the length of the sample (y direction) is given in Fig. 1. It exhibits a strongly peaked field dependence of the magnetic moment M_z.

In order to show that the characteristic peaks are intimately related to the configuration of the in-plane vortex parts, we now describe step by step how vortices enter the film when a field parallel to the y axis is continuously in-

creased. Within the London approximation the thermodynamic potential per unit vortex length is given by [13,14]

$$\tilde{F} = \frac{1}{2\mu_0} \int_{-\infty}^{\infty} dx \int_{-D/2}^{D/2} dz \left[h^2 + \lambda_z^2 \left(\frac{\partial h}{\partial x} \right)^2 \right.$$

$$\left. + \lambda_{xy}^2 \left(\frac{\partial h}{\partial z} \right)^2 - 2\mu_0 h H \right],$$

(1)

where $z = -D/2$ and $z = D/2$ are the top and bottom planes of the film. The total microscopic field $h(x,z)$ along the y axis can be represented as $h(x,z) = h_1(z) + h_2(x,z)$, where the Meissner field $h_1(z)$ is

$$h_1(z) = \frac{\mu_0 H}{\cosh(D/2\lambda_{xy})} \cosh\left(\frac{z}{\lambda_{xy}} \right).$$

(2)

The field $h_2(x,z)$ due to the vortices is calculated by using image vortices in order to ensure zero current across the boundaries of the film. It obeys the equation $h_2 - \lambda_z^2(\partial^2 h_2/\partial x^2) - \lambda_{xy}^2(\partial^2 h_2/\partial z^2) = \phi(x,z)$, where the function $\phi(x,z)$ is periodic in the z direction with a period equal to 2D [summation on N in Eq. (3)]. In the interval $-D/2 < z < 3D/2$, it is given by

$$\phi = \phi_0 \sum_n \delta(x - x_n)[\delta(z - z_n) - \delta(z + z_n - D)],$$

in which the summation on n is over all vortex positions $\{x_n; z_n\}$ inside the film, and ϕ_0 is the flux quantum. The solution can be written as

$$h_2(x,z) = -\frac{i\phi_0}{D} \int_{-\infty}^{\infty} \frac{dq_x}{2\pi} \sum_N \frac{1}{1 + \lambda_z^2 q_x^2 + (\pi N \lambda_{xy}/D)^2} \sum_n \exp\left[iq_x(x - x_n) + i\pi N \left(\frac{z}{D} - \frac{1}{2} \right) \right] \sin\left(\frac{\pi N}{D} z_n + \frac{\pi N}{2} \right).$$

(3)

Substituting Eqs. (2) and (3) into Eq. (1), one obtains, in the limit where $\xi_z \ll D < \lambda_{xy}$, that

$$\tilde{F} = \frac{\phi_0^2}{4\pi\mu_0} \frac{G}{\lambda_{xy}\lambda_z} - \frac{\mu_0 D}{2} \int H^2 dx$$

(4)

with

$$G = \sum_n \left\{ \left[1 + \frac{H^2}{H_{c1}^2} \left[\frac{4z_n^2}{D^2} - 1 \right] \right] \ln\left(\frac{D}{\xi_z} \right) + \ln\left(\frac{\xi_z}{D} + \cos\frac{\pi z_n}{D} \right) \right\}$$

$$+ \frac{1}{2} \sum_{n \neq m} \ln\left\{ \frac{\cosh[\pi\lambda_{xy}(x_n - x_m)/\lambda_z D] + \cos[\pi(z_n + z_m)/D]}{\cosh[\pi\lambda_{xy}(x_n - x_m)/\lambda_z D] - \cos[\pi(z_n - z_m)/D]} \right\}.$$

(5)

The lower critical field H_{c1} is determined by requiring that the energy of a vortex at the surface of the film equals that of a vortex at the center. One finds

$$\mu_0 H_{c1} = \frac{2}{\pi} \frac{\phi_0 \lambda_{xy}}{D^2 \lambda_z} \ln\left(\frac{D}{\xi_z} \right).$$

(6)

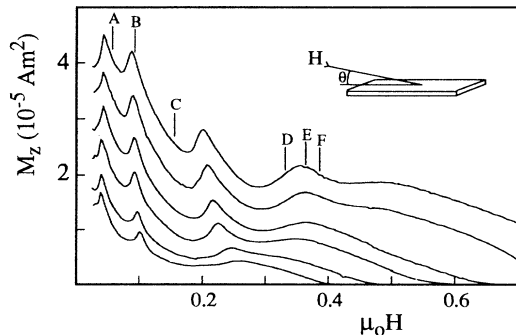By using the experimental values $\lambda_{xy}/\lambda_z = 0.81$, $\xi_z = 13.1$

FIG. 1. Field dependence of the magnetic moment M_z measured with the applied field H at $\theta = 1°$. The curves were obtained at temperatures $T = 1.8$, $T = 2.3$, $T = 2.7$, $T = 3.2$, $T = 3.7$, and $T = 4.1$ K (from top to bottom). The letters A–F refer to the vortex distributions shown in Fig. 3.

nm, and $D = 300$ nm we obtain from Eq. (6) that $\mu_0 H_{c1} = 0.037$ T, which is in good agreement with the first peak position $\mu_0 H_{c1} = 0.040$ T in Fig. 1. The slight difference is due to the uncertainty in D as a result of the thick top and bottom copper layers. The absence of a temperature dependence in the first peak position is a confirmation of Eq. (6) and indicates clearly that we are in the $\lambda_{xy} > D$ limit (unlike the case of Ref. [9]).

For $H > H_{c1}$ vortices begin to enter the sample, and as a result of the Bean-Livingstone barrier, they arrange themselves as a single chain in the middle of the film. As an illustration of the behavior of Eq. (5) the function G is plotted in Fig. 2 for the special case where this chain is allowed to split into a double chain $(z_{2n} = u, z_{2n+1} = -u)$. Clearly there is a characteristic field $H^* = 2.48 H_{c1}$ at which a splitting of the single minimum occurs. Surprisingly the symmetric minima occur almost perfectly at $u = \pm D/6$ and the double chain divides the sample into three equally thick parts. This is by no means a trivial result since the closest vortex-mirror vortex separation is $2D/3$.

In order to explore the behavior of the vortex system at higher fields in more detail we performed a simulation including sixty vortices. They are positioned in a layer of thickness D and width L which is repeated along the x
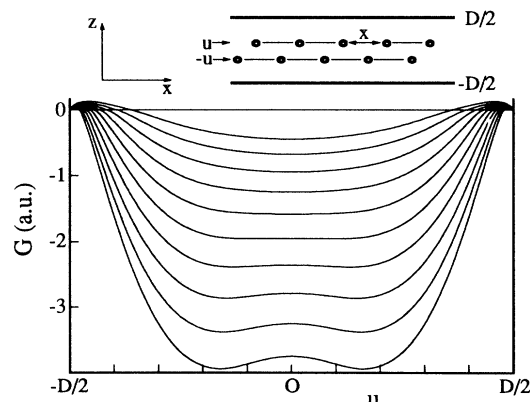
FIG. 2. Normalized Gibbs free energy plotted as a function of the chain splitting u (minimized over the vortex distance x in the chains) for several values of the applied field H. From top to bottom: $H = 1.6$, $H = 1.8$, $H = 2.0$, $H = 2.2$, $H = 2.4$, $H = 2.6$, $H = 2.8$, $H = 3.0$, and $H = 3.2$ (in units of H_{c1}). The splitting of the minimum corresponds to the formation of a double chain state as schematically indicated in the top part of the figure.

axis, making the sample infinite in this direction. The vortex positions $\{x_n, z_n\}$ as well as L (to allow for a change of the vortex density) can vary freely. At a fixed field the influence of changing L and moving each vortex on G can be calculated. Actual displacements of vortices are only allowed when G decreases (essentially $T = 0$ K). After several iterations a stable vortex configuration is reached (local minimum of G) and the field is slightly increased for the next step in the calculation. Figure 3 shows some typical vortex configurations obtained when using $D = 300$ nm and $\xi_z = 13.1$ nm. It indicates clearly that the vortices are organized in chains that split the sample in equally thick parts. Comparison with the experimental data (Fig. 1) shows that on a downward slope (A or C) there is a well defined number of chains. An increase of the external field leads then just to an increasing number of vortices per chain. This process continues on the upward slope (D), but some instability develops as a result of the high vortex density. At the peak position (B or E) a rapid reorganization of the vortices from an n-chain to an $(n+1)$-chain configuration starts. At a slightly higher field the new chains have already been nucleated (F) in a substantial part of the sample. The remarkable correlation between simulation and experimental results shows that the rearrangements of the in-plane vortex system play a decisive role in the determination of the magnetic moment M_z which is essentially due to the vortex kinks. To our knowledge this is the first demonstration of this interrelation although the interaction between "parallel" and "perpendicular" vortex species has recently been discussed in a different context [15,16]. It is important to point out that the formation of chains is not governed by the periodic structure of the multilayer. In the simulation presented here, the multilayer is simply
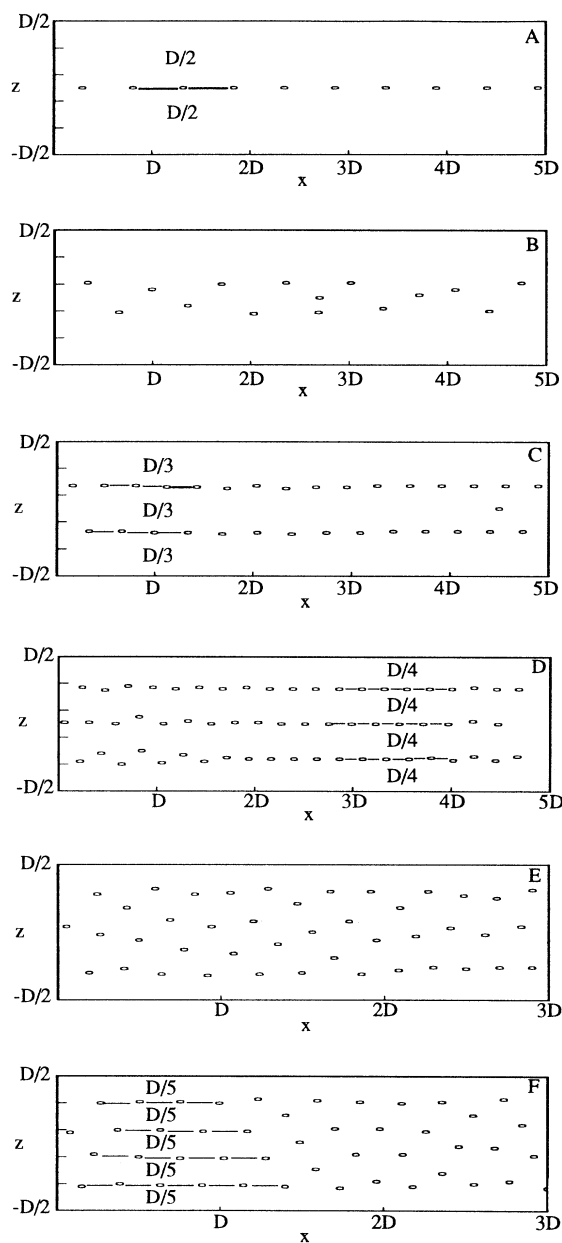

FIG. 3. Vortex distributions obtained in numerical calculations for the six field values indicated by the letters A to F in Fig. 1. (A) $H = 0.068$ T. The single chain is formed above H_{c1}. (B) $H = 0.092$ T. When M_z starts decreasing in the experimental data a reorganization takes place in the simulation. (C) $H = 0.154$ T. As M decreases continuously the vortices are organized in chains in which the density increases with increasing H. The chains split the sample into three equally thick parts. (D) $H = 0.325$ T. On the upward slope in the measurement the triple chain configuration (that splits the sample in four) exhibits instabilities due to the high vortex density in the chains. (E) $H = 0.358$ T. At the peak position another reorganization of the vortex lattice starts taking place. (F) $H = 0.379$ T. At a slightly higher field the quadruple chain appears locally. Note that for clarity an expanded x scale is used for the lower two figures.

treated as an anisotropic superconductor. In fact, addition of an appropriate periodic pinning potential to account for intrinsic pinning has no influence on the general behavior of chain formation (its influence is too small). We used multilayers only to synthesize samples with a large penetration depth so as to be able to satisfy simultaneously the conditions $\lambda_{xy} > D$ and $D \gg \xi_z$.

Figure 1 shows explicitly that the positions H_N of the maxima are virtually temperature independent. However, the number of observed peaks does vary with temperature. This is due to the fact that the upper critical field H_{c2} of a film with thickness $D \gg \xi_z$ is given by the three-dimensional value

$$\mu_0 H_{c2} = \frac{\phi_0}{2\pi\xi_{xy}\xi_z} \propto T_c - T \qquad (7)$$

because the distance between vortex layers is smaller than D. Thus, when the temperature of the sample increases, $H_{c2}(T)$ decreases and the peaks disappear one by one while their positions remain constant (Fig. 1).

In conclusion, torque magnetic moment measurements on artificially layered superconducting films in nearly parallel fields exhibit a series of maxima at specific field strengths H_N. This originates from a vortex chain formation process, which is only possible at small angles ($\theta < 5°$) where large parts of the vortices are parallel to the film plane. The values of H_N show virtually no temperature dependence. However, more maxima are observed at lower temperatures as H_{c2} moves to higher fields. A detailed report on the angular dependence of the peaks in j_c and the influence of the geometry of the sample on the peak heights will be published elsewhere.

[1] M. Tachiki and S. Takahashi, Solid State Commun. **72**, 1083 (1989).

[2] L. N. Bulaevskii, Phys. Rev. B **44**, 910 (1991).

[3] B. I. Ivlev and N. B. Kopnin, J. Low Temp. Phys. **77**, 413 (1989).

[4] A. Barone, A. I. Larkin, and Yu. N. Ovchinnikow, J. Supercond. **3**, 155 (1990).

[5] B. Roas, L. Schultz, and G. Saemann-Ischenko, Phys. Rev. Lett. **64**, 479 (1990).

[6] D. Feinberg and C. Villard, Phys. Rev. Lett. **65**, 919 (1990).

[7] B. I. Ivlev, Yu. N. Ovchinnikow, and V. L. Pokrovsky, Mod. Phys. Lett. B **5**, 73 (1991).

[8] L. N. Bulaevskii, M. Ledvij, and V. G. Kogan, Phys. Rev. B **46**, 366 (1992).

[9] J. Guimpel, L. Civale, F. de la Cruz, J. M. Murduck, and I. K. Schuller, Phys. Rev. B **38**, 2342 (1988).

[10] J. Guimpel, F. de la Cruz, J. Murduck, and I. K. Schuller, Phys. Rev. B **35**, 3655 (1987).

[11] I. Banerjee, Q. S. Yang, C. M. Falco, and I. K. Schuller, Phys. Rev. B **28**, 5037 (1983).

[12] M. Qvarford, K. Heeck, J. G. Lensink, R. J. Wijngaarden, and R. Griessen, Rev. Sci. Instrum. **63**, 5726 (1992). The torque magnetometer used in these experiments does not have a sensitivity of 10^{-12} Nm as in this reference because it is designed to accommodate relatively large samples (up to 20×20 mm^2).

[13] P. G. de Gennes, *Superconductivity of Metals and Alloys* (Benjamin, New York, 1966).

[14] L. Landau and E. Lifchitz, *Electrodynamique des Milieux Continus* (Mir, Moscow, 1969), p. 173.

[15] D. A. Huse, Phys. Rev. B **46**, 8621 (1992).

[16] L. L. Daemen, L. J. Campbell, A. Yu. Simonov, and V. G. Kogan, Phys. Rev. Lett. **70**, 2948 (1993).